Behavior of Disordered Boron Carbide under Stress

Giovanni Fanchini,[1] James W. McCauley,[2] and Manish Chhowalla[1]

[1]*Materials Science and Engineering, Rutgers University, Piscataway, New Jersey 08854, USA*

[2]*ARL, Aberdeen Proving Ground, Aberdeen, Maryland 21005, USA*

(Received 26 December 2005; published 19 July 2006)

Gibbs free-energy calculations based on density functional theory have been used to determine the possible source of failure of boron carbide just above the Hugoniot elastic limit (HEL). A range of B_4C polytypes is found to be stable at room pressure. The energetic barrier for shock amorphization of boron carbide is by far the lowest for the B_{12}(CCC) polytype, requiring only 6 GPa $\approx$ P(HEL) for collapse under hydrostatic conditions. The results clearly demonstrate that the collapse of the B_{12}(CCC) phase leads to segregation of B_{12} and amorphous carbon in the form of 2–3 nm bands along the (113) lattice direction, in excellent agreement with recent transmission electron microscopy results.

DOI: 10.1103/PhysRevLett.97.035502 PACS numbers: 62.20.Mk, 61.66.−f, 64.70.Kb, 82.40.Fp

In today's world, the properties of ceramic materials used for body armor determine the safety and survivability of many people. Although the physics governing the performance of such materials has been an active area of research for years, the theoretical assessment of material properties leading to failure under such conditions has not received significant attention. Typically, a key parameter elucidating the nominal potential of a ceramic as an armor grade material is represented by its Hugoniot elastic limit (HEL) which corresponds to the maximum uniaxial dynamic stress that the material can withstand elastically [1]. However, since the highest velocity threats generally lead to stresses which are higher than the HEL of the commonly available materials, it is almost compulsory for the candidate material to also possess a residual plastic behavior above the HEL. Light weight, wide availability, and processability of the material are also important issues in armor applications.

Boron carbide possesses the highest HEL of ceramic materials (~17–20 GPa), surpassing all of its denser competitors such as silicon carbide and alumina by a factor of 2 [1–3]. Such a property would suggest that boron carbide could withstand high pressures. This, however, has not been observed in laboratory experiments or practice. The small amount of plasticity above the HEL is thought to be the primary reason for failure of boron carbide at lower than expected impact pressures. This behavior is peculiar in dynamically elastic materials, being typical at much lower stresses (<1 GPa) of quartz and glasses [1]. This anomalous and poorly understood glasslike behavior in boron carbide has been the subject of research since its discovery over 70 years ago with most experiments geared towards finding a phase transformation [4].

Although several possibilities such as low fracture toughness and low density have been suggested for the lower than expected performance of boron carbide at high impact velocities and pressures, some recent efforts have provided insights into the dynamic behavior. Vogler *et al.* [5] demonstrated that the collapse at ~20–23 GPa cannot be attributed to a phase transition which they found to occur only above 40 GPa. A phase transition explaining the failure at the HEL must occur [2] at pressures $P \approx P(\mathrm{HEL}) \approx 7.81$ GPa, corresponding to the pressure on the hydrostatic stress-strain curve at the Hugoniot conditions for HEL $\approx$ 17–20 GPa. On the other hand, Chen *et al.* [6] reported observation of shock induced local amorphization in the form of 2–3 nm intragranular bands in boron carbide fragments impacted at velocities >900 m/s (corresponding to HEL = 23.3 GPa). The amorphous bands were absent in fragments impacted at lower velocities. In addition, Ge *et al.* [7] have shown that similar structures (and even in larger amounts) can also be obtained under quasistatic conditions, using nanoindentation or scratching, even if the appearance of the bands obtained after shock is more amorphized, probably due to shear-induced amorphization. Aside from the 2–3 nm amorphous bands, the integrity of the boron carbide crystalline lattice was preserved. This would tend to indicate that the mechanisms for the collapse of the structure at these velocities are not intrinsic of the entire material but spatially localized in specific regions. Their work also eliminated the possibility of any explanations for failure in terms of local melting, rebonding, or influence of twinning and dislocation defects. However, although always found in the collapsed boron carbide, Chen *et al.* [6] were not able to offer an explanation for the origin or the formation mechanism of the amorphous bands.

In this Letter, the determination of the possible root cause for glasslike failure of boron carbide at lower than expected impact pressures and the origin of amorphous bands that accompany the collapse of the structure are reported [8]. Specifically, the B_{12}(CCC) polytype which occurs, as also shown by Werheit *et al.* [9], in hot pressed boron carbide as a minority phase collapses at a much lower pressure than the other making it the weak link that leads to the failure of the entire material.

The boron carbide structure consists of almost regular icosahedra of 12 atoms cross-linked by 3 atomic chains as shown in Fig. 1(a). However, the number n and the location of the carbon atoms in the $B_{12-n}C_n$ icosahedron is not

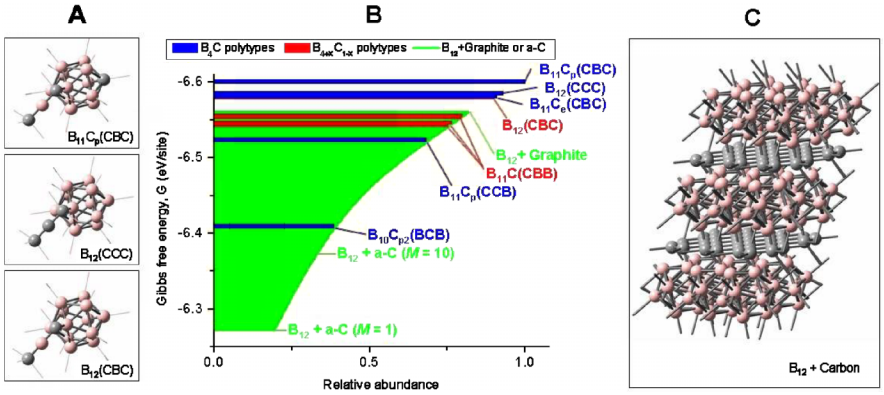

FIG. 1 (color online). (a) Three structures showing the arrangement of icosahedra and chains corresponding to the stoichiometric polytypes $B_{11}C_p$(CBC) and B_{12}(CCC), respectively, and the most energetically favored understoichiometric polytype, B_{12}(CBC). (b) Gibbs energy vs relative abundance of the most significant polytypes in our study. (c) Structure with segregated boron and carbon phases.

known exactly [10]. It can be affected by some degree of randomness, since the 6 equatorial (chain-connected) and the 6 polar (icosahedron-connected) icosahedral sites are indistinguishable. Also the exact sequence of the chain, (CBC) or (CCC), was debated [11]. Therefore, the material could be composed by different *polytypes*, each polytype corresponding to a given chain and icosahderon and being affected by variable degrees of randomness [12]. The stoichiometry may fluctuate. Indeed it is seldom found to be exactly B_4C. Furthermore, the existence of multiple polytypes has been neglected in *ab initio* modeling studies. Instead, it was assumed that one deterministic polytype is entirely responsible for the properties of the material [13].

Therefore, unlike previous theoretical investigations, we have used a multipolytype approach, accounting for the coexistence in the same lattice of different polytypes within a disorder potential ΔV [14]. The necessity of the multipolytype approach is clearly demonstrated in Fig. 1(b) which shows that the Gibbs free energies (G_i) of most of the 20 polytypes we considered in our simulations lie within an energy range comparable to the kinetic energy ($k_B T_s$) available during the synthesis temperature ($T_s > 2000$ K). We used density functional theory (DFT) and different Gaussian basis sets in order to calculate the Gibbs free energies and found negligible basis set dependence [8]. The synthesis temperature is neither instantaneously nor homogeneously reached. Thus, different regions of the material under synthesis experience different energies G, with a probability distribution $f(G) \propto \exp(-G/\Delta V)$ [14] and all polytypes in Fig. 1(b) are synthesized during processing, with a probability $f_i = f(G_i)$.

It should be noted that there is very little difference in lattice parameters amongst the polytypes. Thus all of them can be easily accommodated in the lattice of the most stable polytype, $B_{11}C_p$(CBC) (free energy $G_0 = 6.600$ eV) by introducing minor distortions and a slight loss in free energy per site, $G_i - G_i'$ which is always less than 2% of G_i.

Graphite is often observed in boron carbides and even in B_4C [3]. Our results show that besides the various polytypes, a phase involving separated boron and graphitic carbon can also be accommodated between the icosahedra without a significant loss in Gibbs free energy. The most favored arrangement of the segregated phases (average free energy per site $G(\infty) = 6.560$ eV) involves graphitic layers along the intericosahedral voids corresponding to the reticular (113) plane and slightly displaced B_{12} icosahedra, as shown in Fig. 1(c) [15]. Segregation in the form of graphitic amorphous carbon (a-C) [16] should be less energetically favorable than graphite. However, since the free energy very slowly decreases from graphite to finite aromatic carbon islands, as $G(M) \propto 1.6\text{–}0.3M^{-0.2}$ [16], the difference is still comparable to $\Delta V \gtrsim k_B T_s$ at any size M of the graphitic islands forming a-C. Such considerations are quantified in Fig. 2(a) which describes the coexistence of the various boron carbide polytypes and the segregated boron-carbon phase. Our analysis suggests that, with the disorder potentials ΔV occurring in the actual preparation conditions ($\gtrsim 0.2$ eV), some amount of the segregated boron-carbon phase is unavoidable, as otherwise demonstrated by recent transmission electron microscopy (TEM) analysis [17].

Submitting our structures to increasing hydrostatic pressures at room temperature leads to a decrease in stability of boron carbide with respect segregated boron icosahedra and graphite. Above $P_0 = 6\text{–}7.5$ GPa [vertical lines in Fig. 2(b)], all the polytypes become metastable and the stable arrangement becomes the segregated boron and graphitic layers [18]. This occurs with both polytypes that we find to be the most abundant, $B_{11}C_p$(CBC) and B_{12}(CCC), as shown in the inset of Fig. 2(a). The similarity in behavior of both $B_{11}C_p$(CBC) and B_{12}(CCC) is not surprising when considering that we find, at $P = 10^{-4}$ GPa and 40 GPa, very similar elastic constants for the two polytypes [8] which is also corroborated by the similarity in their calculated vibrational spectra [13]. Nevertheless, this does not mean that a phase transition occurs at $P = P_0$. In order to understand the possibility of such a transition, it is important to estimate as a function of pressure the activation energy barrier separating each boron carbide polytype from the more stable boron-carbon segregated phase.

Let us first observe that the connectivity of the icosahedral sites is very high, each one being connected with 6 other sites, 5 of them pertaining to the icosahedron. We therefore expect very high activation energy to extract an atom from the icosahedron. Our simulations show that the

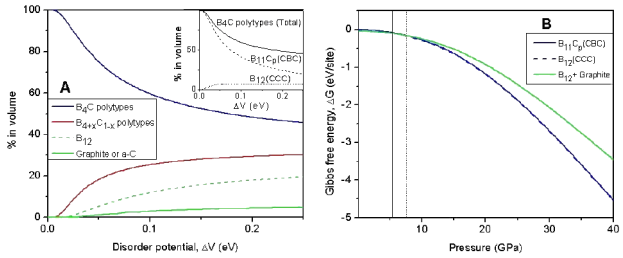

FIG. 2 (color online). (a) The stability of the segregated boron-carbon phase compared to the stability of boron carbide at different disorder potentials, ΔV. (b) Gibbs energies per site of segregated boron and graphite, $B_{12}(CCC)$ and $B_{11}C_p$ (CBC) as a function of pressure calculated via the Birch-Murnaghan equation of state. Lines at 6 GPa (solid line) and 7.5 GPa (dashed line) emphasize the pressures at which the segregated phase becomes more stable than $B_{12}(CCC)$ and $B_{11}C_p$ (CBC).

extraction energy is indeed higher for a polar site than for an equatorial one, while smaller activation energy is required to swap sites within a chain or an icosahedron. This sheds light on the transition path involved in the segregation of $B_{11}C$(CBC) into separated phases of B_{12} graphitic carbon. Quantification of the most energetically favored transition process for the most abundant polytype has been calculated at two pressures and is shown in Fig. 3. For the sake of simplicity the transition process has been divided into four steps, each requiring to overcome an activation energy barrier: (i) migration of the C site in the icosahedron from a polar to an equatorial site [$B_{11}C_p$(CBC) $\rightarrow$ $B_{11}C_e$(CBC)], (ii) migration of the B site in the chain from the central to a boundary site [$B_{11}C_p$(CBC) $\rightarrow$ $B_{11}C_e$(BCC)] with the formation of an electronic defect state, (iii) swapping of the equatorial icosahedral C atom with the boundary B atom in the chain [$B_{11}C_e$(BCC) $\rightarrow$ B_{12}(CCC)], and finally, (iv) the coalescence of the as obtained (CCC) chains along the (113) planes, through a rotation of their axis around the [001] vector. This actually leads the (CCC) chains to form a rectangular lattice of carbon sites, corresponding to a saddle point of the potential energy before their final relaxation into a hexagonal graphitelike lattice.

The energy minima between steps (i)–(iv) in Fig. 3 always correspond to stable B_4C polytypes. Because of very similar force constants, each step can be considered separately and the activation energy of the process corresponds to that of the highest step and hence to the extraction energy of the C_e atom from the icosahedron [step (iii)]. In order to be spontaneous, such an effect requires the icosahedron to become unstable. We have stressed the icosahedra of different compositions at increasing pressures and found the $B_{11}C_e$ icosahedron, the least stable one, to be stable at $P_1 = 40$ GPa. We can therefore conclude that $B_{11}C$(CBC), either with the C site in polar or equatorial position, is at least metastable up to 40 GPa, a value in agreement with the phase transition suggested in the experiments of Vogler *et al* [15].

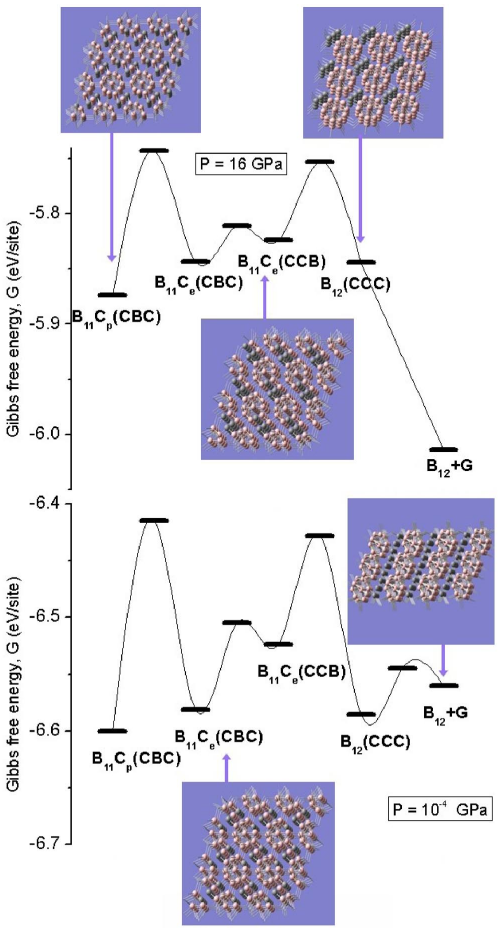

FIG. 3 (color online). Diagrams of the four (i)–(iv) steps required to transform $B_{11}C_p$(CBC) into B_{12} and graphite at 10^{-4} GPa (lower panel) and 16 GPa (upper panel). Only step (iv), the less energetically expensive, is required if the starting carbide has already locally organized as B_{12}(CCC). It can be seen that, at 16 GPa, the B_{12}(CCC) phase has became an unstable point. The thin lines fitting the energy functional are visual aids only.

In contrast, the B_{12}(CCC) polytype does not require any change in the icosahedron structure to transform into separated B_{12} and graphitic phases. Its transition pressure P_2 will then correspond to the energy necessary to rotate the (CCC) chains along the [001] vector and align them along the (113) plane. This requires only a very slight displacement of the boundary C atoms in the chain, which may occur at much lower pressures than P_0. Thus the B_{12}(CCC) polytype becomes unstable at $P_2(\infty) = 6$ GPa $\approx P_0$. This value is only slightly lower than the pressure [P(HEL) $\approx$ 7.81 GPa] occurring on the hydrostatic curve at the failure. Indeed, it should be noted that $P_2(\infty)$ is the lowest limit value for P(HEL) in a material fully composed of (CCC) chains which segregate to form graphitic sheets. Therefore, the failure threshold of boron carbide depends on the presence of the B_{12}(CCC) polytype, since it controls the probability of finding contiguous (CCC) chains and, through the graphitic island size M, the total free energy

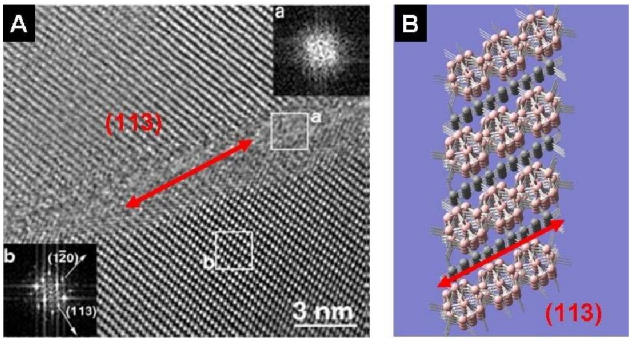

FIG. 4 (color online). (a) High resolution TEM image [Ref. [6]] showing the formation of highly directional 2–3 nm amorphous bands along the (113) plane, and (b) corresponding simulated structure containing the collapsed segregated phases of B_{12} icosahedra and carbon along the (113) direction, in excellent agreement with the TEM results of Ref. [6].

of the as-formed finite graphitic islands. However, since the free energy only weakly decreases from graphite to a-C [16], weak dependency of $P_2(M)$ on the disorder is expected, until an almost complete disappearance of the B_{12}(CCC) polytype occurs. Little dependency of $G(M)$ on disorder as in Ref. [16] explains why the bands are very easily subjected to amorphization, for instance, as a consequence of shear.

Furthermore, $G(M)$ depends on the island size and much less on the distortions of the graphitic rings [16]. Therefore, since the transformation occurs after a shock wave and hence far from equilibrium, the segregation appears in the form of bands of amorphous carbon mixed with B_{12} icosahedra along the (113) plane, as shown in Fig. 4. This is in excellent agreement with the TEM analysis of Chen *et al.* [6] [Fig. 4(a)] and provides a compelling explanation of the relationship between the catastrophic failure of boron carbide and the appearance of the highly directional 2–3 nm amorphous bands. The nucleation of segregated a-C, having glasslike properties (i.e., little elasticity and minimal plasticity), immediately terminates the elastic range and prevents any additional plastic range even if the residual, nonsegregated majority portion of the material would allow it.

Additionally, it is important to notice in Fig. 4(b) that the amorphous region from collapse of the B_{12}(CCC) polytype consists of a mixture of carbon and the boron icosahedra. Thus, the collapsed material should preserve the stoichiometry of the initial material. This is also in agreement with recent electron energy loss spectroscopy (EELS) analysis of the collapsed material which did not detect any change in stoichiometry in the amorphous band [17]. In such bands, according to our model in Fig. 3, the icosahedra have B_{12} composition and the carbon phase is present in an amount determined by the amount of carbon in the pristine B_{12}(CCC) polytype.

We thank Dr. D. E. Niesz and Dr. D. Dandekar for fruitful discussions and Dr. R. A. Haber for support via the Center for Ceramic Research (CCR) at Rutgers University. This project was funded by the Armor Subgroup in CCR and the Academic Excellence Fund at Rutgers.

[1] N. K. Bourne, Proc. R. Soc. Lond. A **458**, 1999 (2002).
[2] G. R. Johnson *et al.*, J. Appl. Phys. **85**, 8060 (1999).
[3] F. Thévenot, J. Eur. Ceram. Soc. **6**, 205 (1990).
[4] R. R. Rigdway, Trans. Am. Eletrochem. Soc. **66**, 117 (1934); D. E. Grady, Mech. Mater. **29**, 181 (1998); D. P. Dandekar, U.S. Army Report No. ARL-TR-2456, 2001 (unpublished).
[5] T. J. Vogler *et al.*, J. Appl. Phys. **95**, 4173 (2004).
[6] M. Chen *et al.*, Science **299**, 1563 (2003).
[7] D. Ge *et al.*, Acta Mater. **52**, 3921 (2004).
[8] See EPAPS Document No. E-PRLTAO-97-051627 for the methods used in the present work. For more information on EPAPS, see http://www.aip.org/pubservs/epaps.html.
[9] H. Werheit *et al.*, J. Solid State Chem. **154**, 79 (2000).
[10] F. Mauri *et al.*, Phys. Rev. Lett. **87**, 085506 (2001); P. Lunca-Popa *et al.*, J. Phys. D **38**, 1248 (2005); Y. Feng *et al.*, Phys. Rev. B **69**, 125402 (2004).
[11] T. M. Duncan, J. Am. Chem. Soc. **106**, 2270 (1984); D. M. Bylander *et al.*, Phys. Rev. B **42**, 1394 (1990).
[12] Polytypes are labeled as $B_{12-n}C_{n,p/e}(XYZ)$ where the subscript (p/e) indicates a random polar/equatorial carbon atom in the icosahedron and (XYZ) is the chain sequence.
[13] R. Lazzari *et al.*, Phys. Rev. Lett. **83**, 3230 (1999).
[14] This approach is a rigorous quantification of the empirical laws generally known as (a) Ostwald and (b) Ostwald-Volmer rules; see A. Bartl *et al.*, Refr. Met. Hard Mat. **14**, 145 (1996). Under this approach, disorder affects the material at an atomistic level during its out-of-equilibrium formation, hence the use of the Gibbs energy per atom in estimating the phase population probabilities.
[15] (113) is neither the softest lattice plane nor the plane where planar defects and twins are generally observed, which is (101). This explains why Chen *et al.*, Ref. [6], found that the direction of the amorphous bands, we here demonstrate to be due to segregation of a-C, is not related to the planar defect directions in the starting material.
[16] J. Robertson, Diam. Rel. Mats. **4**, 297 (1995); Mater. Sci. Eng. R **37**, 129 (2002). Ultimately these works have demonstrated the graphitic island size to be much more important than bond disorder in determining the electronic structure of a-C.
[17] M. W. Chen *et al.*, J. Am. Ceram. Soc. **88**, 1935 (2005).
[18] Segregation of graphitic carbon has also experimentally been observed by Raman, upon nanoindentation experiments by V. Domnich *et al.* Appl. Phys. Lett. **81**, 3783 (2002); and after shock by X. Q. Wan *et al.* Appl. Phys. Lett. **88**, 131905 (2006).